JACS
JOURNAL OF THE AMERICAN CHEMICAL SOCIETY

Article

pubs.acs.org/JACS

Folding Dynamics of Cytochrome *c* Using Pulse Radiolysis

Jungkweon Choi, Mamoru Fujitsuka, Sachiko Tojo, and Tetsuro Majima*

The Institute of Scientific and Industrial (SANKEN), Osaka University, Mihogaoka 8-1, Ibaraki, Osaka 567-0047, Japan

Supporting Information

ABSTRACT: Pulse radiolysis is a powerful method to realize real-time observation of various redox processes, which induces various structural and functional changes occurring in biological systems. However, its application has been mainly limited to studies of the redox reactions of rather smaller biological systems such as DNA because of an undesired reaction due to various free radicals generated by pulse radiolysis. For application of pulse radiolysis to generate plenty of redox reactions of biological systems, selective redox reactions induced by electron pulses have to be developed. In this study, we report that in the presence of the high concentration of the denaturant, guanidine HCl (GdHCl), the selective reduction of the oxidized cytochrome *c* (Cyt *c*) takes place in time scales of a few microseconds by the electron transfer from the guanidine radical that is formed by the fast reaction of e_{aq}^- with GdHCl, consequently leading to folding kinetics of Cyt *c*. By providing insight into the folding dynamics of Cyt *c*, we show that the pulse radiolysis technique can be used to track the folding dynamics of various biomolecules in the presence of a denaturant including GdHCl.

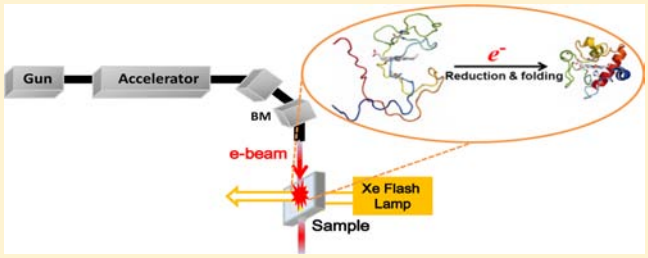

INTRODUCTION

The protein folding process occurring in the biological system has been extensively investigated to understand its structure and function as well as more complex biological phenomena such as the interaction between biomolecules and assembly of complex structures.[1−4] In brief, the protein folding process can be explained by a biphase mechanism: the fast process due to the collapse of the unfolded protein into more compact structures, and the slow phase corresponding to the multistep rearrangement to the native conformation. From this point of view, optical techniques using laser pulses are versatile tools to probe the fast events in the protein folding process. Especially, to track the fast process in the protein folding reaction, the laser-induced electron transfer and the photodissociation reaction of CO ligand have been used to rapidly trigger the protein folding reaction in destabilizing conditions.[5−15] Although the triggering method using the photodissociation reaction of CO has the highest time resolution in following a fast protein folding, it is very difficult to accurately elucidate the structural change of a protein occurring during the folding process because the contribution due to the recombination process between the CO ligand and a protein in the observed signal may be larger than that due to the structural changes of a protein.[14] In contrast to the triggering method using the photodissociation reaction of CO, the triggering method of the laser-induced electron transfer can provide more information for the protein folding dynamics.[5,7−10] In the case of the laser-induced electron transfer method, photosensitizers, such as nicotinamide adenine dinucleotide (NADH), Ru(bipyridine)$_3^{2+}$, or Co(ox)$_3^{3-}$ (ox, $C_2O_4^{2-}$), should be used to inject electrons into a protein.[5,7−10,15] However, photosensitizers, which are used with a high concentration in the reaction system, can influence the protein conformation through the intermolecular interaction between a protein and photosensitizers. In this respect, the pulse radiolysis technique can be proposed as a method more promising than the laser-induced electron transfer method because the powerful reducing agent, hydrated electron (e_{aq}^-), can be directly generated by irradiating the solution with high-energy electrons. Practically, the pulse radiolysis has been extensively used to study the redox reactions of various molecules and materials.[16−21] However, pulse radiolysis also generates free radicals such as OH radical (OH•), H radical (H•), and H_2O_2 in addition to e_{aq}^-;[22] where the numbers in parentheses are the

$$H_2O \rightsquigarrow e_{aq}^-\ (2.8),\ OH\bullet\ (2.8),\ H\bullet\ (0.6),\ H_2O_2\ (0.8),$$

G-value (= number of species formed/100 eV of energy absorbed) indicating the radiation chemical yield. Especially, e_{aq}^- and OH radical (OH•), which are the main species generated by pulse radiolysis, have a high reactivity and substantially induce an undesired reaction with a chemical species involved in the reaction system, whereas the side reaction by free radicals with a low G-value such as the H radical (H•) and H_2O_2 may be negligible, for example, the reduction by e_{aq}^-, oxidation by OH•, etc.[23] Therefore, most studies using pulse radiolysis have been carried out with the scavenger for e_{aq}^- or the OH radical (OH•). In addition, in the presence of a denaturant such as guanidine hydrochloride ($H_2NC(=NH_2)^+NH_2{\cdot}Cl^-$, GdHCl), which is a denaturant frequently used for studying the protein folding reaction, the

Received: May 21, 2012
Published: July 19, 2012

   dx.doi.org/10.1021/ja304904p | *J. Am. Chem. Soc.* 2012, 134, 13430−13435

reactivities of free radicals, especially e_{aq}^- and the OH radical, have never been reported. For this reason, the applicability of pulse radiolysis in the biological system has been limited mainly to studies on the redox reactions of protein and DNA.[17,18,24−26] For studying structural and functional changes occurring in biological systems, therefore, selective redox reactions induced by electron pulses have to be developed.

Here, we demonstrate that the pulse radiolysis technique can be used to track the folding dynamics of a protein (Figure 1). In this study, Cyt *c*, which is a small heme protein (~12 kDa) that serves as an electron carrier in the electron transport chain across a membrane, was used as the target protein. According to a previous report,[9] in the presence of GdHCl ranges between 3.2 and 5.0 M, oxidized Cyt *c* is unfolded, whereas reduced Cyt *c* is folded. (Figure 1b) Therefore, a rapid electron transfer reaction can initiate a folding process. In this report, we clearly show that in the presence of the high concentration of GdHCl, the selective reduction of the oxidized Cyt *c* takes place within time scales of a few microseconds by the electron transfer from the guanidine radical that is formed by the fast reaction of the hydrated electron with guanidine, and then induces the folding reaction of Cyt *c*. This means that the pulse radiolysis technique can be used to track the folding dynamics of various biomolecules in the presence of the denaturant, GdHCl. To our best knowledge, this is the first report for studying the protein folding dynamics using pulse radiolysis.

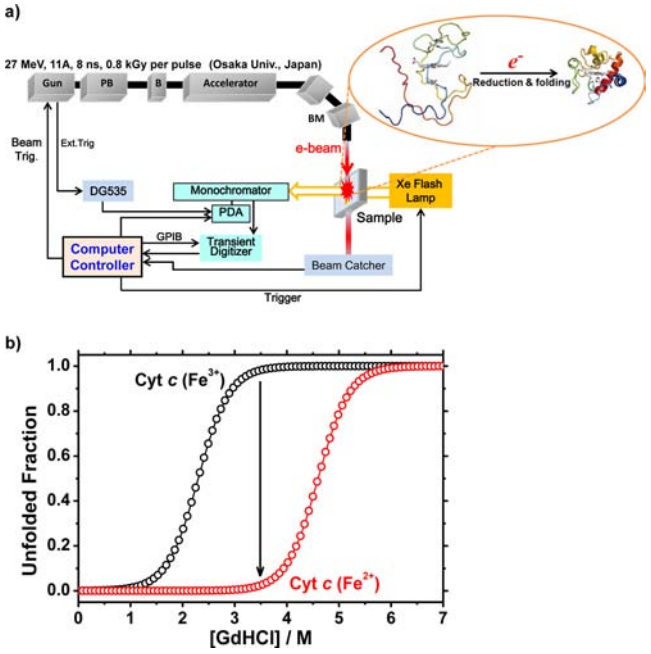

Figure 1. Transient absorption system using pulse radiolysis and folding curves of oxidized and reduced Cyt *c*. (a) Schematic representation of the experimental setup. Pulse radiolysis experiments were performed using an electron pulse (27 MeV, 11 A, 8 ns, 0.8 kGy per pulse) from a linear accelerator at Osaka University. The sample solutions were saturated with Ar gas by bubbling for 15 min at room temperature before irradiation. The kinetic measurements were performed using a nanosecond photoreaction analyzer system (Gun: electric gun, PB: pre-buncher, B: buncher and BM: bending magnet). (b) Folding curves of oxidized and reduced Cyt *c* (Cyt *c* (Fe^{3+}) and Cyt *c* (Fe^{2+}), respectively) as a function of the concentration of GdHCl. These curves were reproduced from ref 9.

EXPERIMENTAL SECTION

Reagents. Equine heart Cyt *c* was purchased from Sigma-Aldrich and used without purification. Guanidine phosphate and methyl viologen (MV^{2+}) were purchased from Nacalai Tesque and TCI Co., respectively, and used without purification.

Preparation of Sample. Cyt *c* solutions (100 mM phosphate buffer, pH 7.0, 375 μM protein, and an appropriate amount of GdHCl, 3.0−4.0 M) were put into a rubber-topped quartz cell and purged with Ar gas for 15 min. The sample was frequently replaced with a fresh sample.

Pulse Radiolysis. Pulse radiolysis experiments were performed using an electron pulse (27 MeV, 11 A, 8 ns, 0.8 kGy per pulse) from a linear accelerator at Osaka University (Figure 1a). The sample solutions were saturated with Ar gas by bubbling for 15 min at room temperature before radiolysis. The monitor light was obtained from a pulsed 450-W Xe arc lamp (Ushio, UXL-451-0), which was operated by a large current pulsed power supply that was synchronized with the electron pulse. The monitor light was passed through an iris with a diameter of 0.3 cm and sent into the sample solution at an intersection perpendicular to the electron pulse. The kinetic measurements were performed using a nanosecond photoreaction analyzer system (Unisoku, TSP-1000). The monitor light passing through the sample was focused on the entrance slit of a monochromator (Unisoku, MD200) and detected with a photomultiplier tube (Hamamatsu Photonics, R2949). The transient absorption spectra were measured using a photodiode array (Hamamatsu Photonics, S3904-1024F) with a gated image intensifier (Hamamatsu Photonics, C2925-01) as a detector.

RESULTS AND DISCUSSION

Pulse Radiolysis of Water in the Absence and Presence of GdHCl. Figure 2a shows the transient absorption spectra obtained by pulse radiolysis of Ar-saturated aqueous solutions buffered with 100 mM phosphate (pH 7). As expected, the broad absorption band around 700 nm due to e_{aq}^- is observed, and the averaged lifetime of e_{aq}^- was determined to be 196 ns by the exponential fitting of the decay profile monitored at 700 nm. However, the transient absorption spectrum obtained by pulse radiolysis of Ar-saturated aqueous solution containing 0.8 M GdHCl buffered with 100 mM phosphate (pH 7) showed two absorption bands around about 350 and 700 nm (Figure 2b). The broad absorption band around 700 nm is easily assigned to the e_{aq}^-. On the other hand, the absorption band with a maximum at 350 nm, depending on the concentration of GdHCl (Figure S1, Supporting Information [SI]), is due to $Cl_2^{\bullet-}$ formed by the reaction of $OH^\bullet$ with chloride ion.[27]

$$Cl^- + OH^\bullet \rightarrow Cl^\bullet + OH^-$$

$$Cl^\bullet + Cl^- \rightarrow Cl_2^{\bullet-}$$

This means that the chloride ion dissociated from GdHCl in this reaction system acts as a scavenger for $OH^\bullet$ generated by pulse radiolysis, implying that the reoxidation of the reduced Cyt *c* induced by $OH^\bullet$ can be diminished. The $Cl_2^{\bullet-}$ is an oxidizing species generated by the reaction of $OH^\bullet$ with a chloride ion and can induce a side reaction with Cyt *c* or various amino acids. In order to test this possibility, we compared two decay profiles of the $Cl_2^{\bullet-}$ generated in 3.5 M GdHCl solutions buffered with 100 mM phosphate (pH 7) and in 3.5 M GdHCl solutions containing 50 μM Cyt *c*. As shown in Figure S2 (SI), two decay profiles are very similar to each other. In addition, the relaxation times of two major components determined from each decay profile are very similar (~0.9 and 4.4 us), although the relaxation time of the

dx.doi.org/10.1021/ja304904p | J. Am. Chem. Soc. 2012, 134, 13430−13435

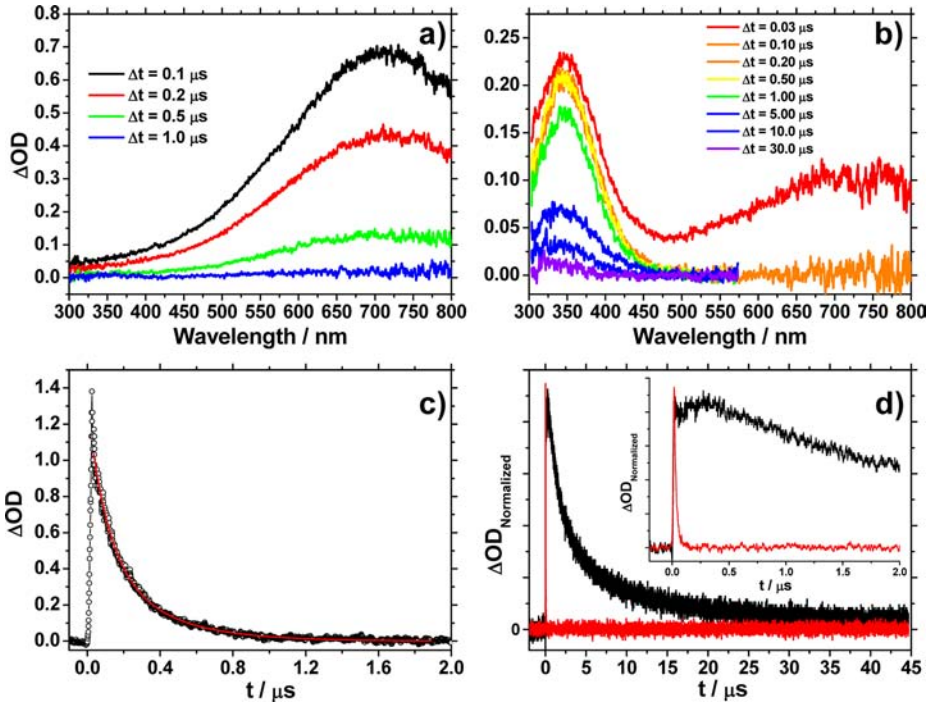

Figure 2. Transient absorption spectra and decay profiles. (a and c) Transient absorption spectra obtained by pulse radiolysis of Ar-saturated aqueous solutions buffered with 100 mM phosphate (pH 7) and the decay profile monitored at 700 nm, respectively. The broad absorption band centered at 700 nm due to the hydrated electron (e_{aq}^-) is observed, and the decay profile is well fitted by a biexponential function, giving the averaged lifetime of 196 ns. Theoretical fits obtained from the fitting analysis are shown in red. (b and d) Transient absorption spectra obtained by pulse radiolysis of Ar-saturated aqueous solutions containing 0.8 M GdHCl solutions buffered with 100 mM phosphate (pH 7) and the decay profiles monitored at 350 (black) and 700 nm (red), respectively. (Inset) Expanded view of early time decay profiles. The absorption band with a maximum at 350 nm, depending on the concentration of GdHCl (Figure S1 [SI]), is due to $Cl_2^{\bullet-}$ formed by the reaction of OH radical with chloride ion. As depicted in this figure, the decay profile monitored at 350 nm showed very complicated features.

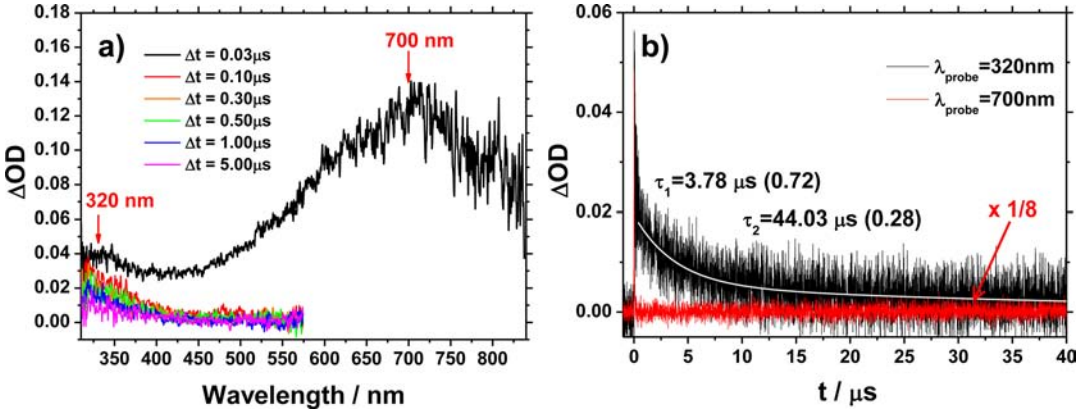

Figure 3. Reaction between e_{aq}^- and the protonated guanidine group. (a and b) Transient absorption spectra obtained by pulse radiolysis in 0.5 M guanidine phosphate ($[H_2NC(=NH)NH_2]\cdot H_3PO_4$) aqueous solutions buffered with 100 mM phosphate (pH 7) and the decay profiles monitored at 320 and 700 nm. The weak band observed at around 320 nm is probably due to guanidine radical formed by the reaction between e_{aq}^- and the protonated guanidine group. The decay profile of the guanidine radical monitored at 320 nm is well fit by a biexponential function, giving the average lifetime of 15.1 μs. Theoretical fit obtained from the fitting analysis are shown in white.

slow component observed in 3.5 M GdHCl solutions containing 50 μM Cyt *c* is longer than that in 3.5 M GdHCl solutions. The longer relaxation time of the slow component observed in 3.5 M GdHCl solutions containing 50 μM Cyt *c* should be due to the changes in the absorption spectra by the folding process of Cyt *c* at the monitoring wavelength (310 nm). (see the section of Reduction and Folding Dynamics of Cyt c for details) These results indicate that most $Cl_2^{\bullet-}$ generated by the reaction of $OH^{\bullet}$ with the chloride ion quickly decays without interacting with Cyt *c*.

On the other hand, it is noteworthy that the decay time of e_{aq}^- generated in the 0.8 M GdHCl solution is significantly fast compared with that observed in water, indicating that e_{aq}^- in the presence of GdHCl quickly reacts with a chemical species involved in this system. It is well-known that e_{aq}^- attacks specifically protonated and unprotonated amines such as pyrrolidine and alkyl amines, and the amine radical formed by the reaction of e_{aq}^- with the protonated (or unprotonated) amine shows the weak absorption band around ~320 nm.[28,29] In addition, as expected from the chemical formula of GdHCl,

dx.doi.org/10.1021/ja304904p | J. Am. Chem. Soc. 2012, 134, 13430−13435

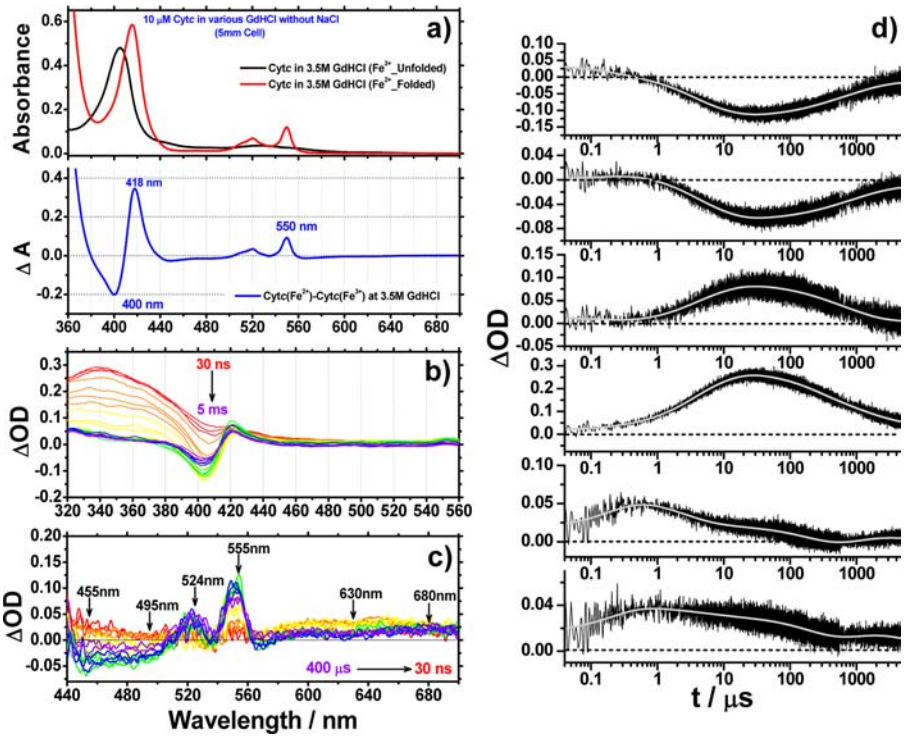

Figure 4. Reduction and folding dynamics of Cyt *c* in 3.5 M GdHCl solutions. (a) The absorption spectra of oxidized and chemically reduced Cyt *c* in 3.5 M GdHCl solution buffered with 100 mM phosphate (pH 7) (top), and the difference spectrum of two absorption spectra (bottom). The absorption spectrum of reduced Cyt *c* was measured in the presence of the reducing agent, sodium dithionite. (b and c) The transient absorption spectra obtained by the pulse radiolysis of Cyt *c* in 3.5 M GdHCl solutions (b and c: transient absorption spectra observed in the Soret- and Q-band region, respectively). In the longer delay time, the transient absorption spectra observed from Cyt *c* showed the same absorption band as the difference spectrum between absorption spectra of reduced and oxidized Cyt *c* in 3.5 M GdHCl solutions, indicating that the selective reduction of the oxidized Cyt *c* takes place in time scales of a few microseconds by the electron transfer from the guanidine radical, and the rapid changes in the visible absorption spectra reflect the folding process of the reduced Cyt *c*. (d) Decay profiles monitored at Q-band region (top to bottom: 455, 495, 524, 555, 630, and 680 nm). The global analysis of all decay profiles show that folding kinetics of Cyt *c* initiated by the electron injection range over a wide time range and are significantly complicated; 4.3×10^5 s^{-1}, 1.3×10^5 s^{-1}, 4.8×10^3 s^{-1}, 1.1×10^3 s^{-1} and 110 s^{-1}. Theoretical fits obtained from the fitting analysis are shown in white.

guanidine exists as the protonated amine form ($H_2NC(=NH_2)^+NH_2$) in the aqueous solutions. This suggests that in this reaction system, the guanidine with a protonated amine group may react with e_{aq}^-.

Guanidine Radical As an Electron Donor. In order to elucidate the reaction of e_{aq}^- with the guanidine group ($H_2NC(=NH_2)^+NH_2$) of GdHCl buffered with 100 mM phosphate (pH 7), we measured the transient absorption spectrum obtained by pulse radiolysis of the aqueous solution containing 0.5 M guanidine phosphate ($[H_2NC(=NH)\text{-}NH_2]\cdot H_3PO_4$). As shown in Figure 3, in addition to the absorption band around 700 nm corresponding to e_{aq}^-, the weak absorption band around 320 nm is observed. According to previous studies,[28,29] this weak band is probably due to a guanidine radical formed by the reaction between e_{aq}^- and the protonated guanidine group. The decay profile of the guanidine radical monitored at 320 nm is well fitted by a biexponential function, giving the average lifetime of 15.1 μs. This result supports that the hydrated electron generated by pulse radiolysis quickly reacts with guanidine, resulting in the formation of the guanidine radical. In other words, this means that the hydrated electron cannot act as the reducing agent for the oxidized Cyt *c*. In order to confirm whether the guanidine radical can act as an electron donor, we have investigated the reduction of methyl viologen (MV^{2+}) in water and 0.5 M guanidine phosphate ($[H_2NC(=NH)\text{-}NH_2]_2\cdot H_3PO_4$) aqueous solutions. In water, the absorption bands of the $MV^{\bullet+}$ generated by the reaction of the hydrated electron with MV^{2+} were observed at 400 and 600 nm. As shown in Figure S2 (SI), $MV^{\bullet+}$ is quickly formed within the pulse width, and then decays. However, although the e_{aq}^- in the 0.5 M guanidine phosphate aqueous solution quickly disappears within the pulse width, $MV^{\bullet+}$ is slowly formed within a few microsecond time scales ($k_{MV+} = 1.57 \times 10^9$ M^{-1} s^{-1}, Figure S3 SI). These results indicate that the e_{aq}^- generated by pulse radiolysis in aqueous solution quickly reacts with the protonated guanidine rather than MV^{2+} because of the high concentration of guanidine phosphate, and then the guanidine radical is quickly formed. Therefore, the slow formation of $MV^{\bullet+}$ is due to the reaction of the guanidine radical with MV^{2+}, implying that the guanidine radical can act as an electron donor (or the reducing agent) in this reaction system.

Consequently, these findings indicate that main radiolysis species are scavenged by the presence of GdHCl and only the reduction process of substrates by the guanidine radical is possible in the present system.

Reduction and Folding Dynamics of Cyt *c*. On the basis of the fundamental experiments, we measured the transient absorption spectra of Cyt *c* in 3.5 M GdHCl solutions buffered with 100 mM phosphate (pH 7). Figure 4a shows the absorption spectra of oxidized and chemically reduced Cyt *c* in 3.5 M GdHCl solutions and the difference spectrum of two

dx.doi.org/10.1021/ja304904p | J. Am. Chem. Soc. 2012, 134, 13430−13435

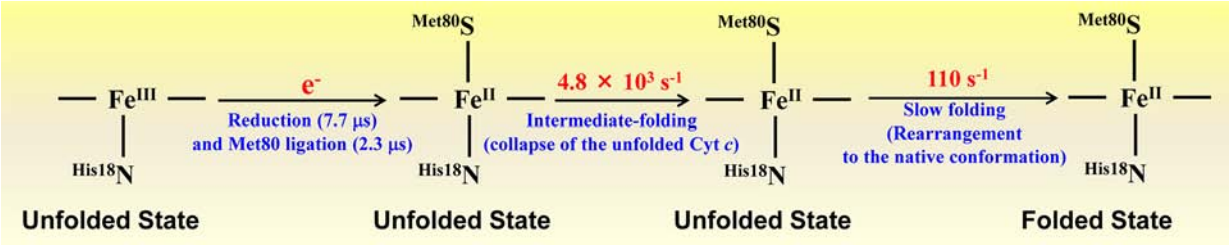

Figure 5. Folding reaction of Cyt *c*. Schematic illustration of the folding reaction of Cyt *c* initiated by the one-electron reduction.

absorption spectra. The transient absorption spectra observed from Cyt *c* at the nanosecond time scale shows the strong and broad absorption band with a maximum at 350 nm due to $Cl_2^{\bullet-}$ formed by the reaction of OH radical with chloride ion. However, in the longer delay time, the transient absorption spectra observed from Cyt *c* showed the same absorption band as the difference spectrum between absorption spectra of reduced and oxidized Cyt *c* in 3.5 M GdHCl solutions. This suggests that the reduction of the oxidized Cyt *c* takes place in time scales of a few microseconds by the electron transfer from the guanidine radical, and the rapid changes in the visible absorption spectra reflect the folding process of the reduced Cyt *c*.

In order to determine the folding kinetics of Cyt *c* induced by the electron transfer, we analyzed the decay profiles monitored at the Soret-band region (Figure S4, SI). However, the spectrum observed in the Soret-band region overlaps with that of $Cl_2^{\bullet-}$ formed by the reaction of OH radical with chloride ion, resulting in great difficulty for elucidating the structural change of a protein occurring during the folding process. Therefore, the absorption spectra in the Q-band region of Cyt *c* were used to determine the folding kinetics of Cyt *c* initiated by the electron injection. The global analysis of all decay profiles monitored at several wavelengths show that folding kinetics of Cyt *c* initiated by the electron injection range over a wide time scale and are significantly complicated; 2.3 ± 0.1 μs (4.3×10^5 s^{-1}), 7.7 ± 0.1 μs (1.3×10^5 s^{-1}), 204 ± 2 μs (4.8×10^3 s^{-1}), 944 ± 10 μs (1.1×10^3 s^{-1}), and 9.4 ± 0.2 ms (110 s^{-1}).

Here, we consider the folding kinetics of Cyt *c* initiated by the one-electron reduction. The spectrum in the Q-band region (500−570 nm) is more sensitive to the heme reduction, whereas the spectrum at the longer wavelength, especially around 695 nm, is more sensitive to ligation states of the heme because the absorption band at 695 nm is due to ligand-to-iron (Met80−heme iron) charge transfer transition.[30,31] As shown in Figure 4d, the decay component of ∼7.7 ± 0.1 μs is observed as a major component in the Q-band region. On the other hand, although the time profiles monitored at 630 and 680 nm in this study are not exactly assignable to the ligand-to-iron charge transfer transitions, the decay component of ∼2.3 ± 0.1 μs is observed as a major component at 630 and 680 nm. Moreover, in the work by Kliger and co-workers, bindings of methionines (Met-80 or Met-65) to the heme iron followed by the photodissociation of the CO ligand take place with a rate of ∼2 μs.[14] They also reported that in the electron-transfer-triggered Cyt *c* folding reaction, reduction of oxidized Cyt *c* and the formation of a His18−Fe(II)−Met ligation occur simultaneously within 5 μs.[5] Considering the previous reports, we tentatively suggest that two fast dynamics (4.3 and 1.3×10^5 s^{-1}) are due to the formation of His18−Fe(II)−Met80 and the reduction of the oxidized Cyt *c*, respectively, indicating that the heme reduction in our system is slower than the binding of Met80 to the heme iron. This result is consistent with that reported by Lee et al.[7]

On the other hand, in our previous study using the fluorescence correlation spectroscopy, we suggested that the collapse of the unfolded yeast iso-1-cytochrome *c* into a compact denatured structure takes place with a rate of 55 μs.[32] Shastry and Roder also reported that the compaction of horse heart Cyt *c* to its first folding intermediate occurs with a time constant of ∼55 μs, independent of initial conditions and heme ligation state.[33] In a study of protein folding triggered by electron transfer using a photosensitizer, Pascher et al. reported that the conformational change of unfolded Cyt *c* into a compact denatured structure occurs with the rate of 40 μs.[9] Werner et al. suggested that the dynamics of ∼30 μs observed from acid-denatured Cyt *c* is due to conformational fluctuation into and out of an intermediate.[34] Although the dynamics of 204 μs (4.8×10^3 s^{-1}) observed in this study is not consistent with those mentioned above, we suggest that the dynamics of 204 μs is due to the intermediate-folding kinetics corresponding to the collapse of the unfolded Cyt *c* into a compact denatured structure. However, we cannot rule out the possibility that the dynamics of 204 μs is attributed to the mis-ligation of the heme such as His33-Fe(II) (or His26-Fe(II)) suggested by Jones et al.[6] In addition, the origin of intermediate folding kinetics of 944 μs (1.1×10^3 s^{-1}) is not clear at present and requires further study.

As mentioned previously, the folding dynamics corresponding to the multistep rearrangement to the native conformation is relatively slow compared to the fast-folding dynamics occurring in the microsecond timescle. Substantially, Pascher et al. reported that the slow-folding dynamics occurs with a rate constant of ∼90 s^{-1} in 2.3 M GdHCl solutions.[9] Nishida et al. reported that the change of the diffusion coefficient due to the folding reaction of Cyt *c* triggered by electron transfer takes place with a rate constant of 22 s^{-1} in 3.5 M GdHCl solutions.[15] These rate constants are consistent with that determined in this study (110 s^{-1}) within an experimental error. Thus, we suggest that the slow dynamics of 110 s^{-1} corresponds to the rearrangement to the native conformation (Figure 5).

■ CONCLUSIONS

Here, we have studied the folding dynamics of Cyt *c* induced by pulse radiolysis. By providing insight into the folding dynamics of Cyt *c*, we show that the pulse radiolysis technique can be used to track the folding dynamics of various biomolecules in the presence of a denaturant including GdHCl. To our best knowledge, this is the first report for studying the protein-folding dynamics using pulse radiolysis, implying that, in addition to the redox reactions of many materials including biomolecules, the conformational dynamics of various bio-

molecules, especially protein folding, can be studied by pulse radiolysis technique in the future. Furthermore, we will investigate the coordination dynamics of the heme accompanied by the folding reaction of Cyt *c* using the time-resolved Raman spectroscopy combined with pulse radiolysis.

■ ASSOCIATED CONTENT

Supporting Information

Additional figures. This material is available free of charge via the Internet at http://pubs.acs.org.

■ AUTHOR INFORMATION

Corresponding Author

majima@sanken.osaka-u.ac.jp

Notes

The authors declare no competing financial interest.

■ ACKNOWLEDGMENTS

We thank the members of the Research Laboratory for Quantum Beam Science of ISIR, Osaka University for running the linear accelerator. This work has been partly supported by a Grant-in-Aid for Scientific Research (Projects 22245022 and others) from the Ministry of Education, Culture, Sports, Science and Technology (MEXT) of Japanese Government. T.M. is grateful for the WCU (World Class University) program funded by the Ministry of Education, Science and Technology through the National Research Foundation of Korea (R31-2008-10035-0) for the support.

■ REFERENCES

(1) Eaton, W. A.; Munoz, V.; Hagen, S. J.; Jas, G. S.; Lapidus, L. J.; Henry, E. R.; Hofrichter, J. *Ann. Rev. Biophys. Biomol. Struct.* **2000**, *29*, 327.
(2) Ivarsson, Y.; Travaglini-Allocatelli, C.; Brunori, M.; Gianni, S. *Eur. Biophys. J.* **2008**, *37*, 721.
(3) Nölting, B. *Protein Folding Kinetics: Biophysical Methods*, 2nd ed.; Springer-Verlag: Berlin, Heidelberg, 2006.
(4) Latypov, R. F.; Cheng, H.; Roder, N. A.; Zhang, J.; Roder, H. *J. Mol. Biol.* **2006**, *357*, 1009.
(5) Chen, E. F.; Wittung-Stafshede, P.; Kliger, D. S. *J. Am. Chem. Soc.* **1999**, *121*, 3811.
(6) Jones, C. M.; Henry, E. R.; Hu, Y.; Chan, C. K.; Luck, S. D.; Bhuyan, A.; Roder, H.; Hofrichter, J.; Eaton, W. A. *Proc. Natl. Acad. Sci. U.S.A.* **1993**, *90*, 11860. 9.
(7) Lee, J. C.; Gray, H. B.; Winkler, J. R. *Proc. Natl. Acad. Sci. U.S.A.* **2001**, *98*, 7760.
(8) Nada, T.; Terazima, M. *Biophys. J.* **2003**, *85*, 1876.
(9) Pascher, T.; Chesick, J. P.; Winkler, J. R.; Gray, H. B. *Science* **1996**, *271*, 1558.
(10) Lee, J. C.; Chang, I. J.; Gray, H. B.; Winkler, J. R. *J. Mol. Biol.* **2002**, *320*, 159.
(11) Latypov, R. F.; Maki, K.; Cheng, H.; Luck, S. D.; Roder, H. *J. Mol. Biol.* **2008**, *383*, 437.
(12) Choi, J.; Yang, C.; Kim, J.; Ihee, H. *J. Phys. Chem. B* **2011**, *115*, 3127.
(13) Cammarata, M.; Levantino, M.; Schotte, F.; Anfinrud, P. A.; Ewald, F.; Choi, J.; Cupane, A.; Wulff, M.; Ihee, H. *Nat. Methods.* **2008**, *5*, 881.
(14) Chen, E.; Wood, M. J.; Fink, A. L.; Kliger, D. S. *Biochemistry* **1998**, *37*, 5589.
(15) Nishida, S.; Nada, T.; Terazima, M. *Biophys. J.* **2004**, *87*, 2663.
(16) Fujitsuka, M.; Majima, T. *J. Phys. Chem. Lett.* **2011**, *2*, 2965.
(17) Vanbuure, Kj; Vangelde, Bf; Wilting, J.; Braams, R. *Biochim. Biophys. Acta* **1974**, *333*, 421.
(18) Kobayashi, K.; Une, H.; Hayashi, K. *J. Biol. Chem.* **1989**, *264*, 7976.
(19) Das, S.; Kamat, P. V. *J. Phys. Chem. B* **1998**, *102*, 8954.
(20) Thomas, M. F.; Li, L. L.; Handley-Pendleton, J. M.; van der Lelie, D.; Dunn, J. J.; Wishart, J. F. *Biores. Technol.* **2011**, *102*, 11200.
(21) Dimitrijevic, N. M.; Bartels, D. M.; Jonah, C. D.; Takahashi, K.; Rajh, T. *J. Phys. Chem. B* **2001**, *105*, 954.
(22) Hart, E. J.; Anbar, M. *The Hydrated Electron*; Wiley-Interscience: New York, 1970.
(23) Elliot, A. J. *Radiat. Phys. Chem.* **1989**, *34*, 753.
(24) Messer, A.; Carpenter, K.; Forzley, K.; Buchanan, J.; Yang, S.; Razskazovskii, Y.; Cai, Y. L.; Sevilla, M. D. *J. Phys. Chem. B* **2000**, *104*, 1128.
(25) Yamagami, R.; Kobayashi, K.; Tagawa, S. *Chemistry* **2009**, *15*, 12201.
(26) Kawai, K.; Kimura, T.; Kawabata, K.; Tojo, S.; Majima, T. *J. Phys. Chem. B* **2003**, *107*, 12838.
(27) Anbar, M.; Thomas, J. K. *J. Phys. Chem.* **1964**, *68*, 3829.
(28) Getoff, N.; Schworer, F. *Radiat. Res.* **1970**, *41*, 1.
(29) Getoff, N.; Schworer, F. *Int. J. Radiat. Phys. Chem.* **1973**, *5*, 101.
(30) Jentzen, W.; Unger, E.; Karvounis, G.; Shelnutt, J. A.; Dreybrodt, W.; SchweitzerStenner, R. *J. Phys. Chem.* **1996**, *100*, 14184. 10.
(31) Dragomir, I.; Hagarman, A.; Wallace, C.; Schweitzer-Stenner, R. *Biophys. J.* **2007**, *92*, 989.
(32) Choi, J.; Kim, S.; Tachikawa, T.; Fujitsuka, M.; Majima, T. *Phys. Chem. Chem. Phys.* **2011**, *13*, 5651.
(33) Shastry, M. C.; Roder, H. *Nat. Struct. Biol.* **1998**, *5*, 385.
(34) Werner, J. H.; Joggerst, R.; Dyer, R. B.; Goodwin, P. M. *Proc. Natl. Acad. Sci. U.S.A.* **2006**, *103*, 11130.